SUPPORTING INFORMATION

Chinese Journal of Structural Chemistry

$ZnMn_3O_7$: A New Layered Cathode Material for Fast-Charging Zinc-Ion Batteries

Ruitao Sun[1,2], Qin Liu[1,2] and Wenzhuo Deng[1]*

[1]*CAS Key Laboratory of Design and Assembly of Functional Nanostructures, and Fujian Key Laboratory of Nanomaterials; State Key Laboratory of Structural Chemistry, Fujian Institute of Research on the Structure of Matter, Chinese Academy of Sciences, Fuzhou 350002, China*
[2]*University of Chinese Academy of Sciences, Beijing 100039, China*

Corresponding author. Email: wzdeng@fjirsm.ac.cn (W. Deng)

Chinese Journal of Structural Chemistry

n Part 1: Theoretical Methods

Spin-polarized structure relaxations and static energy calculations were based on the density functional theory (DFT) implemented in the Vienna ab initio simulation package (VASP).[1] The interaction between core electron and nuclei was treated by the projector-augmented wave (PAW) pseudopotentials,[2] and a cutoff energy of 520 eV was adopted for the plane wave expansion. The Perdew, Burke, and Ernzerhof (PBE)[3] functional of general gradient approximation (GGA) was applied to describe the exchange and correlation interactions. A Gamma-centered Monkhorst-Pack 4 x 4 x 2 *k*-point grid was employed to sample the Brillouin zones (BZ) of $ZnMn_3O_7$. The GGA+U formalism with a Hubbard *U* value of 3.8 eV[4] was exploited to account for the on-site Coulombic interactions of the localized Mn 3*d* electrons. And DFT-D3 proposed by Grimme[5] was used to describe the van der Waals interactions. The optimization of cell dimension and atomic position was completed until the energy changes between each electronic iteration were less than $1x10^{-6}$ eV and the Hellmann-Feynman forces acting on each atom were lower than 0.02 eV/Å.

Chinese Journal of Structural Chemistry

Table S1. lattice parameters of $ZnMn_3O_7$.

Structure	Lattice parameters						
	a (Å)	b (Å)	c (Å)	α (°)	β (°)	γ (°)	V(Å^3)
$ZnMn_3O_7$	7.5842	7.5842	14.2955	90	90	120	705.36

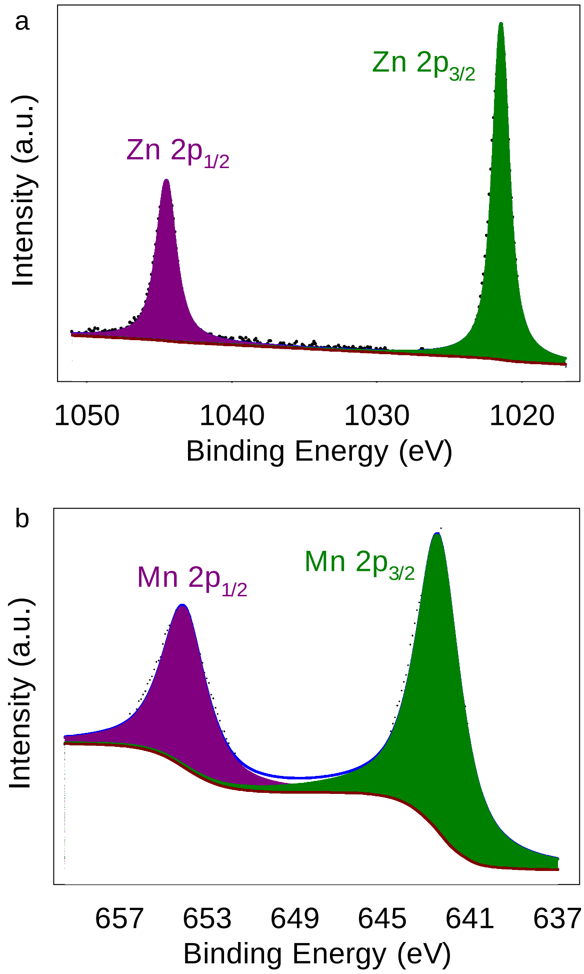

Figure S1. XPS analysis of Zn 2p and Mn 2p.

Table S2. Galvanostatic Cycling Comparisons.

Cathode	Voltage window	Cycle	Capacity retention	Current Density	Reference
$ZnMn_3O_7$	0.8-1.85 V	100	85.3%	0.85 C	This work
δ-MnO_2	1.0-1.8 V	100	34.77%	1.3 C	[6]
$ZnMn_2O_4$	0.8-1.8 V	90	67.87%	0.42 C	[7]
α-MnO_2	1.0-1.8 V	50	65.67%	0.27 C	[8]
α-MnO_2	1.0-1.8 V	75	43.90%	0.27 C	[9]
α-MnO_2	1.0-.85 V	100	53.30%	0.27C	[10]
β-MnO_2	1.0-1.8 V	50	55%	0.33 C	[11]
β-MnO_2	0.8-1.9 V	100	81.80%	0.65 C	[12]
α-Mn_2O_3	1.0-1.9 V	30	79.19%	0.32 C	[13]
α-MnO_2	1.0-1.8 V	100	39.34%	1 C	[14]
δ-MnO_2	1.0-1.8 V	100	44.40%	0.27 C	[15]
α-MnO_2	1.0-1.8 V	100	57.40%	0.33 C	[16]
Mn_3O_4	1.0-1.8 V	30	48%	0.44 C	[17]
$ZnMn_2O_4$	0.8-1.8 V	100	71.30%	1.25 C	[18]
α-MnO_2	1.0-1.9 V	20	92.30%	0.27 C	[19]
T-MnO_2	0.7-2.0 V	50	83.30%	0.5 C	[20]
δ-MnO_2	1.0-1.8 V	100	66.50%	0.33 C	[21]
α-MnO_2	1.0-.85 V	100	89.70%	0.97 C	[10]
α-MnO_2	0.7-2.0 V	30	70%	0.2 C	[22]
γ-MnO_2	1.0-1.8 V	40	63.20%	0.27 C	[23]
O_d-MnO_2	1.0-1.8 V	100	91.90%	0.65 C	[24]
α-MnO_2	0.7-2.0 V	50	56.50%	0.5 C	[20]
$Na_3V_2(PO_4)_3$	0.8-1.7 V	100	83.30%	0.5 C	[25]
ZnHCF	0.8-1.9 V	100	75%	1 C	[26]
LiV_3O_8	0.6-1.2 V	65	74.50%	0.52 C	[27]
$H_3V_2O_8$	0.2-1.6 V	60	84.2%	0.33 C	[28]
CuHCF	0.2-1.2 V	20	77%	0.24 C	[29]

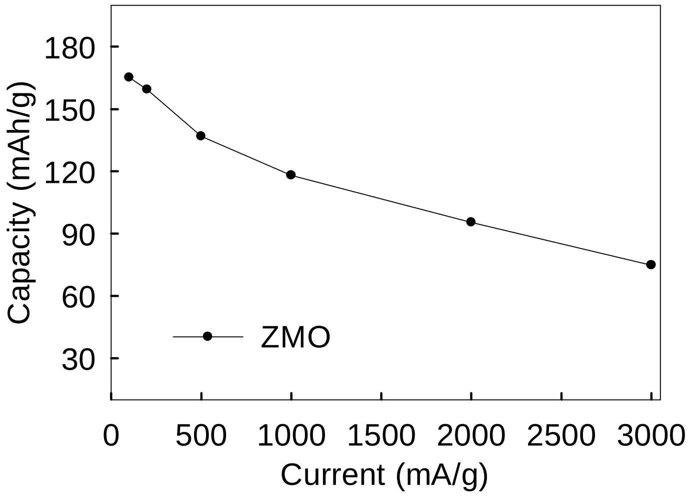

Figure S2. Rate capability of ZMO.

Chinese Journal of Structural Chemistry

Table S3. Rate Capability Comparisons.

Cathode	Rate (C) (mA/g)	Capacity (mAh/g) (mA h/g)	Capacity retention (%)	Reference
$ZnMn_3O_7$	0.1	165	100.00%	This work
	0.2	159	96.51%	
	0.5	137	82.86%	
	1	118	71.53%	
	2	95	57.73%	
	3	75	45.32%	
δ-MnO_2	0.083	208	100.00%	[15]
	0.166	201	96.63%	
	0.333	150	72.12%	
	0.666	92	44.23%	
	1.333	30	14.42%	
	1.666	7	3.37%	
$ZnMn_2O_4$	0.05	148	100.00%	[30]
	0.1	121	81.76%	
	0.2	102	68.92%	
	0.5	90	60.81%	
	1	81	54.73%	
	2	78	52.70%	
α-MnO_2	0.016	353	100.00%	[8]
	0.033	272	77.05%	
	0.066	229	64.87%	
	0.133	200	56.66%	
	0.266	165	46.74%	
	0.533	109	30.88%	
α-MnO_2	0.308	260	100.00%	[31]
	0.616	207	79.62%	
	1.54	161	61.92%	
	3.08	113	43.46%	
α-MnO_2	0.016	323	100.00%	[9]
	0.033	273	84.52%	
	0.066	231	71.52%	
	0.133	197	60.99%	
	0.266	163	50.46%	
	0.533	120	37.15%	
Spinel Mn_3O_4	0.2	232	100.00%	[32]
	0.5	195	84.05%	
	1	163	70.26%	
	2	124	53.45%	
β-MnO_2	0.033	312	100.00%	[11]
	0.066	247	79.17%	
	0.132	193	61.86%	
	0.264	157	50.32%	
	0.528	123	39.42%	
	1.056	86	27.56%	
β-MnO_2	0.2	258	100.00%	[12]
	0.5	213	82.56%	
	1	188	72.87%	
	2	151	58.53%	
α-Mn_2O_3	0.1	137	100.00%	[13]
	0.2	100	72.99%	
	0.3	86	62.77%	
	0.5	74	54.01%	

	1	57	41.61%	
	2	38	27.74%	
δ-MnO_2	0.2	180	100.00%	[6]
	0.4	120	66.67%	
	0.8	75	41.67%	
	1.6	50	27.78%	
α-MnO_2	0.15	405	100.00%	[14]
	0.3	265	65.43%	
	0.6	166	40.99%	
	1.5	85	20.99%	
	3	40	9.88%	
$ZnMn_2O_4$	0.05	238	100.00%	[7]
	0.1	232	97.48%	
	0.2	205	86.13%	
	0.5	167	70.17%	
	1	110	46.22%	
	2	75	31.51%	
β-MnO_2	0.03	285	100.00%	[33]
	0.075	256	89.82%	
	0.15	221	77.54%	
	0.3	193	67.72%	
	0.6	179	62.81%	
	1.2	156	54.74%	
MnO	0.1	267	100.00%	[34]
	0.2	247	92.51%	
	0.4	216	80.90%	
	0.6	172	64.42%	
	0.8	126	47.19%	
	1	95	35.58%	
$ZnMn_2O_4$	0.1	110	100.00%	[18]
	0.3	105	95.45%	
	0.5	100	90.91%	
	0.8	90	81.82%	
	1	70	63.64%	
	2	50	45.45%	
α-MnO_2	0.1	350	100.00%	[35]
	0.2	315	90.00%	
	1	230	65.71%	
	2	162	46.29%	
	3	150	42.86%	
T-MnO_2	0.15	NA	100.00%	[20]
	0.3	NA	92.00%	
	0.9	NA	71.00%	
δ-MnO_2	0.1	225	100.00%	[21]
	0.2	200	88.89%	
	0.3	180	80.00%	
	0.4	163	72.44%	
	0.5	150	66.67%	
	1	120	53.33%	
δ-MnO_2	0.012	110	100.00%	[36]
	0.03	98	89.09%	
	0.06	89	80.91%	
	0.15	65	59.09%	
	0.30	30	27.27%	
α-MnO_2	0.1	242.3	100.00%	[10]

	0.3	176.4	72.80%	
	0.5	151.5	62.53%	
	1	104.3	43.05%	
	3	58.9	24.31%	
O_d-MnO_2	0.2	345	100.00%	[24]
	0.5	298	86.38%	
	1	235	68.12%	
	2	170	49.28%	
$Na_3V_2(PO_4)_3$	0.06	65.4	100.00%	[25]
	0.12	60.4	92.35%	
	0.18	56.8	86.85%	
	0.3	52.5	80.28%	
	0.6	45.5	69.57%	
	0.9	39.1	59.79%	
ZnHCF	0.06	65	100.00%	[26]
	0.12	60	92.35%	
	0.18	57	86.85%	
	0.3	53	80.27%	
	0.6	46	69.57%	
	0.9	39	59.79%	
$Na_{0.33}V_2O_5$	0.1	367.1	100.00%	[37]
	0.2	253.7	69.11%	
	0.5	173.4	47.24%	
	0.8	145.3	39.58%	
	1	137.5	37.46%	
	2	96.4	26.26%	
LiV_3O_8	0.016	256	100.00%	[27]
	0.033	230	89.84%	
	0.066	211	82.42%	
	0.133	188	73.44%	
	0.266	148	57.81%	
	0.533	79	30.86%	
$Zn_3V_2O_7(OH)_2\cdot 2H_2O$	0.05	200	100.00%	[38]
	0.1	166	83.00%	
	0.3	145	72.50%	
	0.5	122	61.00%	
	0.8	105	52.50%	
	1	84	42.00%	
$K_2V_8O_{21}$	0.3	247	100.00%	[39]
	0.5	226	91.50%	
	1	183	74.09%	
	2	139	56.28%	
NaV_3O_8	0.1	372	100.00%	[40]
	0.2	320	86.02%	
	0.5	277	74.46%	
	1	241.5	64.92%	
	2	205	55.11%	
V_2O_5	0.05	242	100.00%	[41]
	0.1	217	89.67%	
	0.2	192	79.34%	
	0.5	171	70.66%	
	1	156	64.46%	

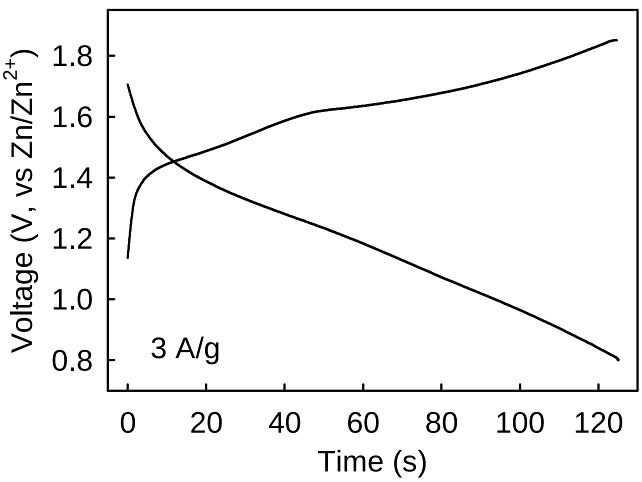

Figure S3. The time-voltage profiles of the fast-charge.

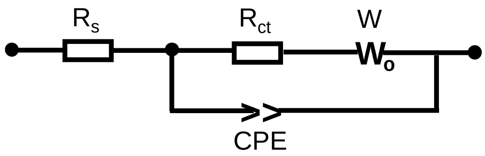

Figure S4. The equivalent circuit model.

Chinese Journal of Structural Chemistry

Table S4. The Resistance Derived from EIS.

	Resistance/Ω	Pristine	After 3 cycles
$ZnMn_3O_7$	R_s	1.355	1.786
	R_{ct}	47.67	45.08

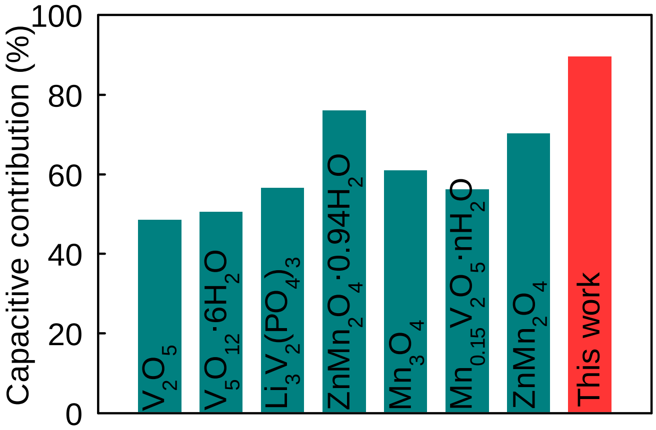

Figure S5. Comparison of capacitive contributions.[7, 42-47]

n REFERENCES

(1) Kresse, G.; Furthmuller, J. Efficient iterative schemes for ab initio total-energy calculations using a plane-wave basis set. *Phys. Rev. B* **1996**, 54, 11169-11186.

(2) Chen, D.; Taylor, K. P.; Hall, Q.; Kaplan, J. M. The neuropeptides FLP-2 and PDF-1 act in concert to arouse caenorhabditis elegans locomotion. *Phys. Rev. B* **2016**, 204, 1151-1159.

(3) Perdew, J. P.; Burke, K.; Ernzerhof, M. Generalized gradient approximation made simple. *Phys. Rev. Lett.* **1996**, 77, 3865-3868.

(4) Wang, L.; Maxisch, T.; Ceder, G. Oxidation energies of transition metal oxides within theGGA+Uframework. *Phys. Rev. B* **2006**, 73, 195107.

(5) Grimme, S.; Antony, J.; Ehrlich, S.; Krieg, H. A consistent and accurate ab initio parametrization of density functional dispersion correction (DFT-D) for the 94 elements H-Pu. *J. Chem. Phys*. **2010**, 132, 154104.

(6) Khamsanga, S.; Pornprasertsuk, R.; Yonezawa, T.; Mohamad, A. A.; Kheawhom, S. Delta-MnO_2 nanoflower/graphite cathode for rechargeable aqueous zinc ion batteries. *Sci. Rep*. **2019**, 9, 8441.

(7) Chen, L.; Yang, Z.; Qin, H.; Zeng, X.; Meng, J. Advanced electrochemical performance of $ZnMn_2O_4$/N-doped graphene hybrid as cathode material for zinc ion battery. *J. Power Sources* **2019**, 425, 162-169.

(8) Alfaruqi, M. H.; Gim, J.; Kim, S.; Song, J.; Jo, J.; Kim, S.; Mathew, V.; Kim, J. Enhanced reversible divalent zinc storage in a structurally stable α-MnO_2 nanorod electrode. *J. Power Sources* **2015**, 288, 320-327.

(9) Alfaruqi, M. H.; Islam, S.; Gim, J.; Song, J.; Kim, S.; Pham, D. T.; Jo, J.; Xiu, Z.; Mathew, V.; Kim, J. A high surface area tunnel-type α-MnO_2 nanorod cathode by a simple solvent-free synthesis for rechargeable aqueous zinc-ion batteries. *Chem. Phys. Lett*. **2016**, 650, 64-68.

(10) Wu, B.; Zhang, G.; Yan, M.; Xiong, T.; He, P.; He, L.; Xu, X.; Mai, L. Graphene scroll-coated alpha-MnO_2 nanowires as high-performance cathode materials for aqueous Zn-ion battery. *Small* **2018**, 14, e1703850.

(11) Islam, S.; Alfaruqi, M. H.; Mathew, V.; Song, J.; Kim, S.; Kim, S.; Jo, J.; Baboo, J. P.; Pham, D. T.; Putro, D. Y.; Sun, Y.-K.; Kim, J. Facile synthesis and the exploration of the zinc storage mechanism of β-MnO_2 nanorods with exposed (101) planes as a novel cathode material for high performance eco-friendly zinc-ion batteries. *J. Mater. Chem. A* **2017**, 5, 23299-23309.

(12) Zhang, N.; Cheng, F.; Liu, J.; Wang, L.; Long, X.; Liu, X.; Li, F.; Chen, J. Rechargeable aqueous zinc-manganese dioxide batteries with high energy and power densities. *Nat. Commun*. **2017**, 8, 405.

(13) Jiang, B.; Xu, C.; Wu, C.; Dong, L.; Li, J.; Kang, F. Manganese sesquioxide as cathode material for multivalent zinc ion battery with high capacity and long cycle life. *Electrochim. Acta* **2017**, 229, 422-428.

(14) Guo, X.; Li, J.; Jin, X.; Han, Y.; Lin, Y.; Lei, Z.; Wang, S.; Qin, L.; Jiao, S.; Cao, R. A hollow-structured manganese oxide cathode for stable Zn-MnO_2 batteries. *Nanomaterials-Basel* **2018**, 8, 301.

(15) Alfaruqi, M. H.; Gim, J.; Kim, S.; Song, J.; Pham, D. T.; Jo, J.; Xiu, Z.; Mathew, V.; Kim, J. A layered δ-MnO_2 nanoflake cathode with high zinc-storage capacities for eco-friendly battery applications. *Electrochem. Commun*. **2015**, 60, 121-125.

(16) Guo, C.; Tian, S.; Chen, B.; Liu, H.; Li, J. Constructing α-MnO_2@PPy core-shell nanorods towards enhancing electrochemical behaviors in aqueous zinc ion battery. *Mater. Lett*. **2020**, 262, 127180.

(17) Zhu, C.; Fang, G.; Zhou, J.; Guo, J.; Wang, Z.; Wang, C.; Li, J.; Tang, Y.; Liang, S. Binder-free stainless steel@Mn_3O_4 nanoflower composite: a high-activity aqueous zinc-ion battery cathode with high-capacity and long-cycle-life. *J. Mater. Chem. A* **2018**, 6, 9677-9683.

(18) Chen, L.; Yang, Z.; Qin, H.; Zeng, X.; Meng, J.; Chen, H. Graphene-wrapped hollow $ZnMn_2O_4$ microspheres for high-performance cathode materials of aqueous zinc ion batteries. *Electrochim. Acta* **2019**, 317, 155-163.

(19) Nam, K. W.; Kim, H.; Choi, J. H.; Choi, J. W. Crystal water for high performance layered manganese oxide cathodes in aqueous rechargeable zinc batteries. *Energy Environ. Sci*. **2019**, 12, 1999-2009.

(20) Lee, J.; Ju, J. B.; Cho, W. I.; Cho, B. W.; Oh, S. H. Todorokite-type MnO_2 as a zinc-ion intercalating material. *Electrochim. Acta* **2013**, 112, 138-143.

(21) Guo, C.; Liu, H.; Li, J.; Hou, Z.; Liang, J.; Zhou, J.; Zhu, Y.; Qian, Y. Ultrathin δ-MnO_2 nanosheets as cathode for aqueous rechargeable zinc ion battery. *Electrochim. Acta* **2019**, 304, 370-377.

(22) Lee, B.; Lee, H. R.; Kim, H.; Chung, K. Y.; Cho, B. W.; Oh, S. H. Elucidating the intercalation mechanism of zinc ions into alpha-MnO_2 for rechargeable zinc batteries. *Chem. Commun*. **2015**, 51, 9265-9268.

(23) Alfaruqi, M. H.; Mathew, V.; Gim, J.; Kim, S.; Song, J.; Baboo, J. P.; Choi, S. H.; Kim, J. Electrochemically induced structural transformation in a γ-MnO_2 cathode of a high capacity zinc-ion battery system. *Chem. Mater*. **2015**, 27, 3609-3620.

(24) Xiong, T.; Yu, Z. G.; Wu, H.; Du, Y.; Xie, Q.; Chen, J.; Zhang, Y. W.; Pennycook, S. J.; Lee, W. S. V.; Xue, J. Defect engineering of oxygen-deficient manganese oxide to achieve high-performing aqueous zinc ion battery. *Adv. Energy Mater*. **2019**, 9, 1803815.

(25) Li, G.; Yang, Z.; Jiang, Y.; Jin, C.; Huang, W.; Ding, X.; Huang, Y. Towards polyvalent ion batteries: A zinc-ion battery based on NASICON structured $Na_3V_2(PO_4)_3$. *Nano Energy* **2016**, 25, 211-217.

(26) Zhang, L.; Chen, L.; Zhou, X.; Liu, Z. Towards High-Voltage Aqueous Metal-Ion Batteries Beyond 1.5 V: The zinc/zinc hexacyanoferrate system. *Adv. Energy Mater*. **2015**, 5, 1400930.

(27) Alfaruqi, M. H.; Mathew, V.; Song, J.; Kim, S.; Islam, S.; Pham, D. T.; Jo, J.; Kim, S.; Baboo, J. P.; Xiu, Z.; Lee, K.-S.; Sun, Y.-K.; Kim, J. Electrochemical zinc intercalation in lithium vanadium oxide: a high-capacity zinc-ion battery cathode. *Chem. Mater.* **2017**, 29, 1684-1694.

(28) He, P.; Quan, Y.; Xu, X.; Yan, M.; Yang, W.; An, Q.; He, L.; Mai, L. High-performance aqueous zinc-ion battery based on layered $H_2V_3O_8$ nanowire cathode. *Small* **2017**, 13, 1702551.

(29) Jia, Z.; Wang, B.; Wang, Y. Copper hexacyanoferrate with a well-defined open framework as a positive electrode for aqueous zinc ion batteries. *Mater. Chem. Phys*. **2015**, 149-150, 601-606.

(30) Zhang, N.; Cheng, F.; Liu, Y.; Zhao, Q.; Lei, K.; Chen, C.; Liu, X.; Chen, J. Cation-deficient spinel $ZnMn_2O_4$ cathode in $Zn(CF_3SO_3)_2$ electrolyte for rechargeable aqueous zn-ion battery. *J. Am. Chem. Soc*. **2016**, 138, 12894-12901.

(31) Pan, H.; Shao, Y.; Yan, P.; Cheng, Y.; Han, K. S.; Nie, Z.; Wang, C.; Yang, J.; Li, X.; Bhattacharya, P.; Mueller, K. T.; Liu, J. Reversible aqueous zinc/manganese oxide energy storage from conversion reactions. *Nat. Energy* **2016**, 1, 16039.

(32) Hao, J.; Mou, J.; Zhang, J.; Dong, L.; Liu, W.; Xu, C.; Kang, F. Electrochemically induced spinel-layered phase transition of Mn_3O_4 in high performance neutral aqueous rechargeable zinc battery. *Electrochim. Acta* **2018**, 259, 170-178.

(33) Liu, M.; Zhao, Q.; Liu, H.; Yang, J.; Chen, X.; Yang, L.; Cui, Y.; Huang, W.; Zhao, W.; Song, A.; Wang, Y.; Ding, S.; Song, Y.; Qian, G.; Chen, H.; Pan, F. Tuning phase evolution of β-MnO_2 during microwave hydrothermal synthesis for high-performance aqueous Zn ion battery. *Nano Energy* **2019**, 64, 103942.

(34) Wang, J.; Wang, J.-G.; Liu, H.; You, Z.; Wei, C.; Kang, F. Electrochemical activation of commercial MnO microsized particles for high-performance aqueous zinc-ion batteries. *J. Power Sources* **2019**, 438, 226951.

(35) Zhao, Z.; Zhao, J.; Hu, Z.; Li, J.; Li, J.; Zhang, Y.; Wang, C.; Cui, G. Long-life and deeply rechargeable aqueous Zn anodes enabled by a multifunctional brightener-inspired interphase. *Energy Environ. Sci*. **2019**, 12, 1938-1949.

(36) Han, S.-D.; Kim, S.; Li, D.; Petkov, V.; Yoo, H. D.; Phillips, P. J.; Wang, H.; Kim, J. J.; More, K. L.; Key, B.; Klie, R. F.; Cabana, J.; Stamenkovic, V. R.; Fister, T. T.; Markovic, N. M.; Burrell, A. K.; Tepavcevic, S.; Vaughey, J. T. Mechanism of Zn Insertion into Nanostructured δ-MnO_2: A Nonaqueous Rechargeable Zn Metal Battery. *Chem. Mater*. **2017**, 29, 4874-4884.

(37) He, P.; Zhang, G.; Liao, X.; Yan, M.; Xu, X.; An, Q.; Liu, J.; Mai, L. Sodium ion stabilized vanadium oxide nanowire cathode for high-performance zinc-ion batteries. *Adv. Energy Mater*. **2018**, 8, 1702463.

(38) Xia, C.; Guo, J.; Lei, Y.; Liang, H.; Zhao, C.; Alshareef, H. N. Rechargeable aqueous zinc-ion battery based on porous framework zinc pyrovanadate intercalation cathode. *Adv. Mater*. **2018**, 30, 1705580.

(39) Tang, B.; Fang, G.; Zhou, J.; Wang, L.; Lei, Y.; Wang, C.; Lin, T.; Tang, Y.; Liang, S. Potassium vanadates with stable structure and fast ion diffusion channel as cathode for rechargeable aqueous zinc-ion batteries. *Nano Energy* **2018**, 51, 579-587.

(40) Wan, F.; Zhang, L.; Dai, X.; Wang, X.; Niu, Z.; Chen, J. Aqueous rechargeable zinc/sodium vanadate batteries with enhanced performance from simultaneous insertion of dual carriers. *Nat. Commun*. **2018**, 9, 1656.

(41) Hu, P.; Yan, M.; Zhu, T.; Wang, X.; Wei, X.; Li, J.; Zhou, L.; Li, Z.; Chen, L.; Mai, L. Zn/V_2O_5 aqueous hybrid-ion battery with high voltage platform and long cycle life. *ACS Appl. Mater. Interfaces* **2017**, 9, 42717-42722.

(42) Zhang, N.; Dong, Y.; Jia, M.; Bian, X.; Wang, Y.; Qiu, M.; Xu, J.; Liu, Y.; Jiao, L.; Cheng, F. Rechargeable aqueous Zn-V_2O_5 battery with high energy density and long cycle life. *ACS Energy Lett.* **2018**, 3, 1366-1372.

(43) Zhang, N.; Jia, M.; Dong, Y.; Wang, Y.; Xu, J.; Liu, Y.; Jiao, L.; Cheng, F. Hydrated layered vanadium oxide as a highly reversible cathode for rechargeable aqueous zinc batteries. *Adv. Funct. Mater.* **2019**, 29, 1807331.

(44) Li, C.; Yuan, W.; Li, C.; Wang, H.; Wang, L.; Liu, Y.; Zhang, N. Boosting $Li_3V_2(PO_4)_3$ cathode stability using a concentrated aqueous electrolyte for high-voltage zinc batteries. *Chem. Commun.* **2021**, 57, 4319-4322.

(45) Wu, T. H.; Liang, W. Y. Reduced intercalation energy barrier by rich structural water in spinel $ZnMn_2O_4$ for high-rate zinc-ion batteries. *ACS Appl. Mater. Interfaces* **2021**, 13, 23822-23832.

(46) Sun, M.; Li, D. S.; Wang, Y. F.; Liu, W. L.; Ren, M. M.; Kong, F. G.; Wang, S. J.; Guo, Y. Z.; Liu, Y. M. Mn_3O_4@NC composite nanorods as excellent cathode for rechargeable aqueous zn-ion battery. *ChemElectroChem* **2019**, 6, 2510-2516.

(47) Geng, H.; Cheng, M.; Wang, B.; Yang, Y.; Zhang, Y.; Li, C. C. Electronic structure regulation of layered vanadium oxide via interlayer doping strategy toward superior high-rate and low-temperature zinc-ion batteries. *Adv. Funct. Mater.* **2019**, 30, 1907684.